Available online at www.sciencedirect.com
ScienceDirect
Journal of Photochemistry and Photobiology A: Chemistry 182 (2006) 288–295
Journal of Photochemistry and Photobiology A:Chemistry
www.elsevier.com/locate/jphotochem

Reverse electron transfer at the interface of semiconductor film in dye-sensitized solar cells

Masatoshi Yanagida *, Kazuhiro Sayama, Kazuyuki Kasuga, Mitsuhiko Kurashige, Hideki Sugihara **

Energy Technology Research Institute, National Institute of Advanced Industrial Science and Technology, 1-1-1 Higashi, AIST-Tsukuba Central 5, Tsukuba, Ibaraki 305-8565, Japan

Abstract

The photovoltaic performance of dye-sensitized solar cells (DSCs) based on nanocrystalline TiO_2 films with co-absorbed $[NBu_4]_2$[*cis*-Ru(Hdcbiq)$_2$(NCS)$_2$] (**BQ**; $[NBu_4]^+$ = tetrabutyl ammonium cation; H_2dcbiq = 4,4′-dicarboxy-2,2′-biquinoline) and $[NBu_4]_2$[*cis*-Ru(Hdcbpy)$_2$(NCS)$_2$] (**N719**; H_2dcbpy = 4,4′-dicarboxy-2,2′-bipyridine) has been investigated. The excited state (E^*_{ox}) of **BQ** is more positive than that of **N719** and is comparable to the conduction band edge (E_{cb}) of the TiO_2. The short circuit photocurrent density (J_{sc}) and open circuit photovoltage (V_{oc}) decreased with increasing adsorbed **BQ** on the TiO_2 when **N719** and **BQ** were co-adsorbed on the TiO_2. The dark current of DSCs with co-absorbed **BQ** and **N719** increased with increasing adsorbed **BQ** on the TiO_2. Therefore, we propose that an electron injected from **N719** to TiO_2 and then trapped by **BQ** subsequently reacted with I_2. The photovoltaic performance of DSCs with co-adsorbed **N719** and **BQ** can be explained by reverse electron transfer from TiO_2 to I_2 through **BQ**.

Keywords: Dye-sensitized solar cell; Ruthenium complex; Nanocrystalline TiO_2; Reverse electron transfer; Electron transport

1. Introduction

Metal complex sensitizers and organic sensitizers have been synthesized and characterized with the goal of improving the solar-to-electric energy conversion efficiencies (η) of dye-sensitized solar cells (DSC) that are based on nanocrystalline TiO_2 films [1–14]. The main strategy in the design of sensitizers is to enhance the spectrum response over a wide wavelength region and to maintain a sufficient thermodynamic driving force for electron injection from a sensitizer to TiO_2 and electron transfer from I^- to the oxidized sensitizer [4–14]. Researchers have also focused on reverse electron transfer from TiO_2 to I_2 because reverse electron transfer from TiO_2 to I_2 is related to the open circuit photovoltage (V_{oc}) and the dark current of DSCs [15–27]. The V_{oc} is known to decrease with increasing dark current. The present work describes reverse electron transfer from TiO_2 to I_2 in DSCs.

The mechanism of reverse electron transfer from TiO_2 to I_2 has been investigated in DSCs based on nanocrystalline TiO_2 sensitized with $[NBu_4]_2$[*cis*-Ru(Hdcbpy)$_2$(NCS)$_2$] (**N719**; H_2dcbpy = 4,4′-dicarboxy-2,2′-bipyridine), which is a typical sensitizer [2,3,15–27]. This research has focused on the basic understanding of reverse electron transfer from TiO_2 to I_2, namely, nano-structure dependent reverse electron transfer and electron diffusion in TiO_2. Sensitizer-dependent reverse electron transfer has recently been reported in nanocrystalline TiO_2 electrodes [26,28–31]. When coumarin dyes (NKX-2587, 2677, and 2697) containing a thiophene group are adsorbed on TiO_2, the dark current in coumarin dye-sensitized TiO_2 depends on the number of thiophene units in the molecule, and is larger than the dark current in **N719**-sensitized TiO_2 [30]. By investigating electron transport in TiO_2, we found that the conduction band edge (E_{cb}) of TiO_2 sensitized with **N719** is approximately 50 mV more negative than that of TiO_2 sensitized with $[NBu_4]_2$[Ru(Htcterpy)(NCS)$_3$] (H_3tcterpy = 4,4′,4″-tricarboxy-2,2′:6′,2″-terpyridine) [31]. The dark current of DSCs sensitized with ruthenium complexes increases with a positive shift in the reduction potential of the ruthenium complexes [14,32]. Recently, we found that electrons injected into a TiO_2 film co-absorbed with **N719**

* Corresponding author. Tel.: +81 298 61 4641; fax: +81 298 61 6771.
** Corresponding author.
E-mail address: m.yanagida@aist.go.jp (M. Yanagida).

1010-6030/$ – see front matter © 2006 Elsevier B.V. All rights reserved.
doi:10.1016/j.jphotochem.2006.06.010

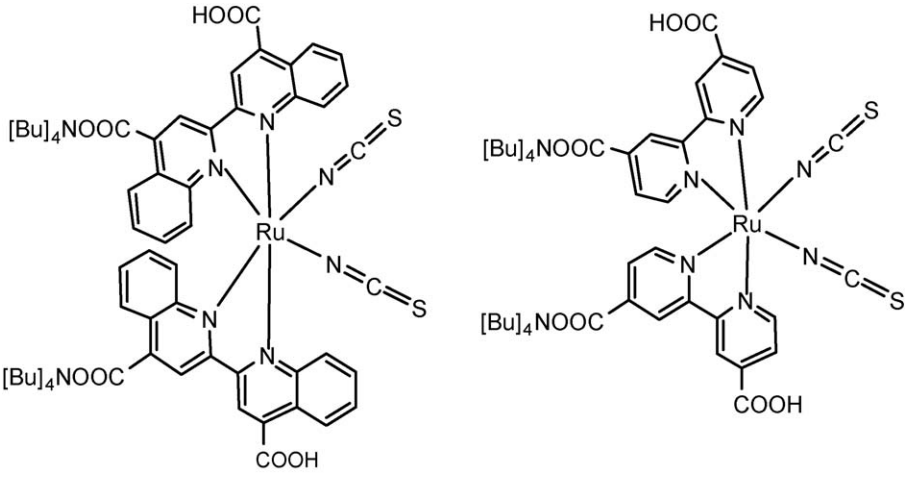

Fig. 1. Ruthenium complexes **BQ**, $[NBu_4]_2$[*cis*-Ru(Hdcbiq)$_2$(NCS)$_2$] ($[NBu_4]^+$ = tetrabutyl ammonium cation; H_2dcbiq = 4,4′-dicarboxy-2,2′-biquinoline), and **N719**, $[NBu_4]_2$[*cis*-Ru(Hdcbpy)$_2$(NCS)$_2$] (H_2dcpy = 4,4′-dicarboxy-2,2′-bipyridine).

and $[NBu_4]_2$[*cis*-Ru(Hdcbiq)$_2$(NCS)$_2$] (**BQ**; H_2dcbiq = 4,4′-dicarboxy-2,2′-biquinoline) react with I_2 predominantly through **BQ** [32]. The excited state (E^*_{ox}) of **BQ** is more positive than that of **N719** and is comparable to the conduction band edge (E_{cb}) of TiO_2 [10,11,14]. To evaluate reverse electron transfer in detail, we investigated the photovoltaic performances of nanocrystalline TiO_2 film electrodes with co-absorbed **N719** and **BQ** (Fig. 1).

2. Experimental procedures

2.1. Materials

All materials were reagent grade and were used as received unless otherwise noted. The $[NBu_4]_2$[*cis*-Ru(Hdcbiq)$_2$(NCS)$_2$] (**BQ**) was synthesized according to the literature method [11]. The $[NBu_4]_2$[*cis*-Ru(Hdcbpy)$_2$(NCS)$_2$] (**N719**) was purchased from Solaronix S.A. (Lausanne, Switzerland).

2.2. Preparation of samples

Nanocrystalline TiO_2 colloids and pastes were prepared as described previously [33]. The paste was printed on conductive glass plates (F-doped SnO_2, Nippon Sheet Glass Co., Tokyo, Japan, 8–10 $\Omega\,cm^{-2}$) using a screen-printing machine before calcination at 525 °C for 2 h [27]. The thickness (d) of the TiO_2 films was measured with a Tencor Alpha Step 500 profiler (KLA-Tencor Japan Ltd., Kanagawa, Japan). The geometric surface area of the TiO_2 film electrode was measured with a microscope (Nikon, Tokyo, Japan, model C-PS). The geometric surface area and d values for the TiO_2 were approximately 0.26 cm^2 and 6.5 μm, respectively [32]. The actual inner surface areas of the TiO_2 films were estimated by Brunauer–Emmett–Teller measurements. The specific surface area of the nanocrystalline TiO_2 films was estimated to be 91 $m^2\,g^{-1}$. The diameter of the particles was approximately 17 nm. The density of the nanocrystalline TiO_2 film (1.2 $g\,cm^{-3}$) was calculated by measuring the weight of the film (0.26 cm^2 × 28 μm). The roughness factor of the TiO_2 (d = 7 μm) was 745. The TiO_2 electrodes were optically transparent.

The bare TiO_2 films were annealed at 450 °C for 1 h and dipped in ethanolic dye solution at a concentration of 3×10^{-4} M at room temperature for 20 h. The amounts of **BQ** and **N719** (Γ in mol cm^{-2}) co-adsorbed on the TiO_2 film were controlled by changing the ratio between **BQ** and **N719** in the dipping solutions. The Γ values were determined by desorbing the dye from the TiO_2 film into a 0.01 M NaOH 1:1 (v/v) ethanol–water solution and measuring the absorbance ($A(\lambda)$) of the solutions at wavelength (λ) with a UV–vis absorption spectrometer (Shimadzu, Kyoto, Japan, UV3101PC). The amount of adsorbed **BQ** and **N719** were calculated according to the literature method [32]. The Γ values for **BQ** and **N719** are designated as Γ_{BQ} and Γ_{N719}, respectively.

2.3. Methods

A UV–vis absorption spectrometer (Shimadzu, Kyoto, Japan, UV3101PC) and a potentiostat (Solartron, Durham, UK, SI1280B) were used for spectroelectrochemical measurements. The UV–vis absorption spectra of the TiO_2 electrodes sensitized with dye were measured in an electrolyte consisting of 0.1 M $[NBu_4]ClO_4$ in acetonitrile. The thickness of the TiO_2 films for absorption spectra was around 2 μm.

Photoelectrochemical measurements were performed in a sandwich-type two-electrode cell consisting of a dye-coated TiO_2 film electrode, a polypropylene film spacer (60 μm), an electrolyte solution, and a platinum (Pt) film counter electrode. The electrolyte solution in the cell consisted of 0.5 M 4-*tert*-butylpyridine, 0.6 M (1,2-dimethyl-3-propyl)imidazolium iodide, 0.05 M I_2, and 0.1 M LiI in acetonitrile.

The photovoltaic measurements were conducted by using a Xe lamp light source simulating the AM 1.5 spectrum (Wacom, Tokyo, Japan, WXS-80C-3, 100 mW cm^{-2}). The incident monochromatic photon-to-current conversion efficiency (IPCE) was measured by using IPCE measurement system (Bunko Keiki Co., Tokyo, Japan, CED99-W) with a monochro-

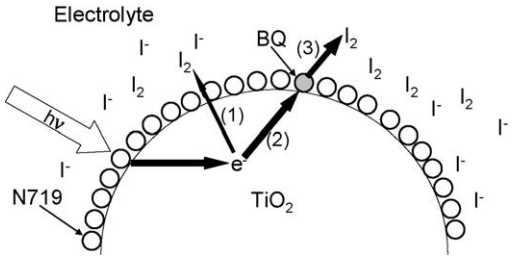

Fig. 2. Proposed mechanism for reverse electron transfer from TiO_2 to I_2 through **BQ**.

matic Xe lamp. Intensity-modulated photovoltage spectroscopy (IMVS) measurements at open circuit were carried out using a combination of low-intensity-modulated illumination from a green diode laser (Cobolt Co., Stockholm, Sweden, Samba, 532 nm, 50 mW) and constant-bias light illumination from a Xe lamp (Ushio, Tokyo, Japan, UXL-500D-O), attenuated if necessary with a neutral-density filter. The laser-light illumination was modulated with an acoustic optical modulator (Isomet Co., Springfield, USA, 1205C-1). The intensity of the modulated light was decreased so that the photocurrent of the cell under the modulated-light irradiation was 11% of that under the constant-bias light irradiation. IMPS and IMVS measurements were performed using an impedance analyzer (Solartron, Durham, UK, Model 1260 impedance/gain-phase analyzer) to drive the laser and to analyze the photocurrent and photovoltage responses.

3. Model

The proposed mechanism of sensitizer-dependent recombination is shown in Fig. 2 [32]. When TiO_2 is covered with **N719**, the injected electron reacts with I_2 at the TiO_2/electrolyte interface (step 1). The normal reverse electron transfer (step 1) at **N719**-sensitized TiO_2 takes place thorough **N719** on TiO_2 or at bare TiO_2 surface. When ruthenium complex **BQ** is co-adsorbed on TiO_2 sensitized with **N719**, **BQ** in the ground state traps the injected electrons (step 2), which then react with I_3^- (step 3). We defined the dye absorption ratio (ρ_{BQ}) as $\rho_{BQ} = \Gamma_{BQ}/(\Gamma_{BQ} + \Gamma_{N719})$. In addition, the relative cross section of electron trapping by a sensitizer on TiO_2 is defined as σ_{trap}. When the value of σ_{trap} for **N719** corresponds to the cross section for step 1 and is hypothetically defined to be 1, the possibility (P_{trap}) of an encounter with **BQ** adsorbed on the surface is given by

$$P_{trap} = \frac{\sigma_{trap}\Gamma_{BQ}(1-S)}{\Gamma_{N719} + \sigma_{trap}\Gamma_{BQ}} \quad (1)$$

where S is the ratio of the amount of reduced **BQ** to Γ_{BQ} ($0 \le S \le 1$). If an electron moves randomly and is trapped by a sensitizer on nanocrystalline TiO_2, the σ_{trap} value of **BQ** is expected to be 1. Therefore, the possibility of an encounter with **BQ** adsorbed on the surface is $\rho_{BQ}(1-S)$. Eq. (1) can be simplified by the following assumptions. We assumed that an electron trapped by **BQ** on TiO_2 cannot be released from the trap site. In addition, because polypyridyl ligands of metal complexes tend to interact with I_2 [34], we assumed that the rate constant of the electron transfer from **BQ** to I_2 is much larger than the rate constant (k_{trap}) of electron trapping from the conduction band to **BQ**. Therefore, S is small ($S \ll 1$). Thus, P_{trap} can be described as $\sigma_{trap}\Gamma_{BQ}/\Gamma_{N719} + \sigma_{trap}\Gamma_{BQ}$. When DSCs are illuminated from the conductive glass side, the concentration (n) of the injected electrons in TiO_2 can be described as a function of the distance (x) from the conductive glass/nanocrystalline TiO_2 interface to an area parallel to the interface in the nanocrystalline TiO_2 ($0 < x < d$, see Fig. 2) and time (t). The electron density ($n(x,t)$), which depends on the absorption of light and on electron transport, is given by the following continuity equation [32]:

$$\frac{\partial n(x,t)}{\partial t} = D\frac{\partial^2 n}{\partial x^2} - \frac{n}{\tau} - k_{trap} n P_{trap} + \alpha_{N719}\eta_{inj} I_0 e^{-\alpha_s x} \quad (2)$$

$$\frac{\partial S}{\partial t} = k_{trap} n \frac{P_{trap}}{\Gamma_{BQ}} - k_{rv} S \quad (3)$$

$$\alpha_s = \alpha_{N719} + \alpha_{BQ} \quad (4)$$

where α_{N719} is the absorption coefficient of **N719** on TiO_2, α_{BQ} the absorption coefficient of **BQ** on TiO_2, τ the apparent electron lifetime (s) in the nanocrystalline TiO_2 sensitized with **N719**, D the apparent electron diffusion coefficient ($cm^2\,s^{-1}$) in **N719**-sensitized TiO_2, η_{inj} the electron injection yield from a dye to TiO_2, and I_0 is the incident photon flux corrected for reflection loss.

The absorption coefficients ($\alpha(\lambda)$) are given by

$$\alpha(\lambda) = 2.302 A(\lambda) d^{-1}. \quad (5)$$

The $\alpha_s(\lambda)$ is calculated from the A(530 nm) of the TiO_2 with adsorbed **N719** and the TiO_2 with adsorbed **BQ**, and the Γ values of the TiO_2 films.From Eq. (2), the apparent electron lifetime (τ_{app}) and the apparent diffusion coefficient (D_{app}) in the TiO_2 films with co-adsorbed sensitizers are given by

$$\tau_{app} = \frac{1}{1/\tau + k_{trap} P_{trap}} \quad (6)$$

$$D_{app} = D. \quad (7)$$

Eq. (2) can be written as

$$\frac{\partial n(x,t)}{\partial t} = D_{app}\frac{\partial^2 n}{\partial x^2} - \frac{n}{\tau_{app}} + \alpha_{N719}\eta_{inj} I_0 e^{-\alpha_s x}. \quad (8)$$

Eq. (8) has been used to analyze DSCs [15–27,35]. The diffusion length L ($L = \sqrt{D_{app}\tau_{app}}$ in cm) can be expressed as

$$L = \sqrt{D_{app}\tau_{app}} = \frac{L_{N719}}{\sqrt{1 + k_{trap} P_{trap}\tau}} = \frac{L_{N719}}{\sqrt{1 + \frac{k_{trap}\tau\rho_{BQ}}{1+(\sigma_{trap}-1)\rho_{BQ}}}} \quad (9)$$

where L_{N719} is the diffusion length in **N719**-sensitized TiO_2. The electron density $n(0,t)$ at the conductive glass can be described as [35]

$$n(0,t) = n_0 \exp\left(\frac{qV}{mkT}\right) \quad (10)$$

where V is the bias, q the quantity of charge on the electron (C), k the Boltzmann's constant (J K^{-1}), T the absolute temperature (K), m the ideality factor, and n_0 is the electron density in the dark (cm^{-3}). The n_0 value is also given by

$$n_0 = N_c \exp\left(\frac{q(E_{cb} - E(I_3^-/I^-))}{kT}\right) \quad (11)$$

where N_c is the density of states in the conduction band and $E(I_3^-/I^-)$ is the redox potential of I_3^-/I^-.

The photocurrent density ($J_{photocurrent}$) is given by

$$J_{photocurrent} = qD_{app}\frac{\partial n(0,\infty)}{\partial x}. \quad (12)$$

At the steady state ($\partial n(x,t)/\partial t = 0$), $n(x,\infty)$ can be solved by using Eq. (7) for $\partial n(d,t)/\partial x = 0$. The $J_{photocurrent}$ can be expressed as a function of L as follows:

$$J_{photocurrent} = -qD_{app}\frac{n_0}{L}\exp\left(\frac{qV}{mkT}\right)\tanh\left(\frac{d}{L}\right) + \frac{q\eta_{inj}I_0\alpha_{N719}L}{2\cosh(d/L)}\left[\frac{\alpha_s\exp(-\alpha_s d) - (1/L)\exp(-d/L)}{1/L - \alpha_s} + \frac{\alpha_s\exp(-\alpha_s d) + (1/L)\exp(d/L)}{1/L + \alpha_s}\right]. \quad (13)$$

When I_0 equals 0 in Eq. (13), the dark current density is given by

$$J_{dark} = -qD_{app}\frac{n_0}{L}\exp\left(\frac{qV}{mkT}\right)\tanh\left(\frac{d}{L}\right). \quad (14)$$

From Eq. (14), J_{dark} increases with decreasing L. $J_{photocurrent}$ is also represented by

$$J_{photocurrent} = J_{dark} + J_{sc}. \quad (15)$$

When $J_{photocurrent} = 0$, the open circuit photovoltage (V_{oc}) is given by

$$V_{oc} = \frac{mkT}{q}\ln\left(\frac{J_{sc}}{J_{dark}(V=0)}\right) \quad (16)$$

$$J_{dark}(V=0) = \frac{qD_{app}n_0}{L}\tanh\left(\frac{d}{L}\right). \quad (17)$$

From Eqs. (13)–(15), the relationship between the incident monochromatic photon-to-current conversion efficiency (IPCE) and L is given by

$$IPCE = \frac{J_{sc}}{qI_0} = \frac{\eta_{inj}\alpha_{N719}L}{2\cosh(d/L)}\left[\frac{(1/L)\exp(d/L) + \alpha_s\exp(-\alpha_s d)}{1/L + \alpha_s} - \frac{(1/L)\exp(-d/L) - \alpha_s\exp(-\alpha_s d)}{1/L - \alpha_s}\right]. \quad (18)$$

According to Eq. (18), the IPCE values increase with increasing L.

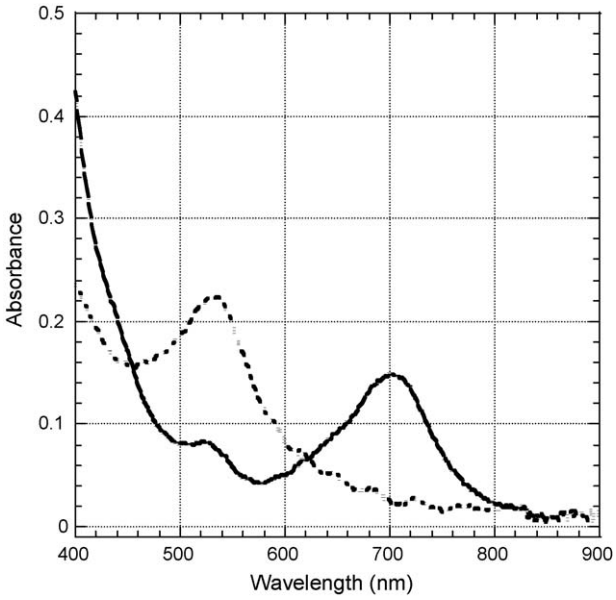

Fig. 3. UV–vis absorption spectra of **N719** (- - -) and **BQ** (—) adsorbed on a TiO_2 film electrode in 0.1 M $[NBu_4]ClO_4$ acetonitrile solution at an electrode potential of −0.1 V versus SCE.

4. Results and discussion

4.1. Adsorption of *N719* and *BQ* on TiO_2

The Γ values of **BQ** and **N719** adsorbed TiO_2 films at $d = 7\,\mu m$ were 9.2×10^{-8} and 8.8×10^{-8} mol cm^{-2}, respectively. If the dye completely covered the TiO_2, then **BQ** and **N719** both occupied an area of approximately 135 $Å^2$ [32], a value that is in good agreement with the value reported by Shklover et al. [36]. The number of adsorbed dye molecules per particle was estimated to be 670 molecules [32]. The Γ_{N719} is linearly related to the volume ratio (R_{N719}) of the **N719** solution to the total volume in a dipping solution. The ρ_{BQ} is also linearly related to the R_{N719}. These results show that the adsorption equilibrium constant of **BQ** is comparable to that of **N719**, assuming simple Langmuir adsorption.

UV–vis absorption spectra of **BQ** and **N719** adsorbed on a TiO_2 film in 0.1 M $[NBu_4]ClO_4$ acetonitrile electrolyte solution are shown in Fig. 3. The spectra of **BQ** and **N719** adsorbed on a TiO_2 film at −0.1 V versus SCE show peaks at 700 and 530 nm, which are similar to the spectra of **BQ** and **N719** adsorbed on a TiO_2 film in air [11]. The peak at 700 nm represents a red shift of approximately 50 nm from the peak for **BQ** in DMF or ethanol solution, which indicates that **BQ** is sensitive to the surrounding conditions. The Γ can also be calculated from $A(700\,nm) = 0.15$ of **BQ** on TiO_2 film to be 1.3×10^{-8} mol cm^{-2} on the supposition that the molar absorption coefficient ($\varepsilon_{BQ}(700\,nm)$) of **BQ** at 700 nm equals 12,000 $M^{-1}\,cm^{-1}$. The Γ can also be calculated from $A(530\,nm) = 0.23$ of **N719** on a TiO_2 film to be 1.7×10^{-8} mol cm^{-2} on the supposition that the molar absorption coefficient ($\varepsilon_{N719}(530\,nm)$) of **N719** at 530 nm equals 13,800 $M^{-1}\,cm^{-1}$. The $\varepsilon_{BQ}(530\,nm)$ was calculated to be 6400 $M^{-1}\,cm^{-1}$ because $A(530\,nm)$ of **BQ** was 0.08. The ratio of the absorption coefficients ($\alpha_{BQ}(\alpha_{N719} + \alpha_{BQ})^{-1}$) at 530 nm

was calculated to be 0.17 at $\rho_{BQ} = 0.3$ when for TiO_2 films with co-adsorbed **BQ** and **N719**. Light absorption by **BQ** on a TiO_2 film reduces the solar-to-electric energy conversion efficiency of DSCs and cannot be neglected at $\rho_{BQ} \geqq 0.3$.

4.2. Short-circuit photocurrent (J_{sc})

Plots of IPCE(530 nm) versus ρ_{BQ} for the DSCs based on nanocrystalline TiO_2 films with co-adsorbed **BQ** and **N719** are shown in Fig. 4(a and b). The IPCE values were experimentally estimated from the following equation:

$$\mathrm{IPCE}(\lambda) = \frac{1}{q}\left(\frac{J_{sc}(\lambda)}{I_0(\lambda)}\right) \times 100 = \mathrm{APCE}(\lambda) \times \mathrm{LHE}(\lambda) \quad (19)$$

where LHE(λ) is the light-harvesting efficiency and APCE(λ) is the absorbed photon-to-current conversion efficiency. LHE(λ) is defined as

$$\mathrm{LHE}(\lambda) = 1 - 10^{-A(\lambda)} \quad (20)$$

where $A(\lambda)$ is expressed as

$$A(\lambda) = 1000\varepsilon\Gamma \quad (21)$$

The IPCE values of the cells based on **BQ**- and **N719**-sensitized TiO_2 were 0.6% and 75% at 530 nm, respectively. IPCE(530 nm) values decreased with increasing ρ_{BQ}. The LHE values at 532 nm for $\rho_{BQ} \leq 0.30$ were calculated to be 0.90. The IPCE values would be expected to be linearly related to LHE if the APCE values were 100%. However, the IPCE value for the solar cells with $\rho_{BQ} = 0.30$ was 22% at 530 nm, which was much smaller than expected. That is, the IPCE value decreased substantially even when a small amount (for example, $\rho_{BQ} = 0.04$) of **BQ** was co-adsorbed with **N719** on the TiO_2. Electron-transfer or energy-transfer interactions between **BQ** and **N719** seem to have been negligible [32]. We speculated that the η_{inj} does not depend on ρ_{BQ}. Therefore, an electron injected from **N719** to the TiO_2 reacted with I_2 through **BQ** on the TiO_2.

The L value of **N719**-sensitized solar cells at short circuit was assumed to be 37 μm [32]. Using the least-squares fit of the plot of IPCE versus ρ_{BQ}, k_{trap} and σ_{trap} were estimated to be 1800 $cm^3\ s^{-1}$ and 1.1, respectively. The best value of k_{trap} was estimated in the least-squares fit when σ_{trap} was changed from 0.1 to 20. We assumed the transmittance of the conductive glass was 80% at 530 nm because the maximum value of IPCE at 530 nm was 80% [14]. The L value calculated from Eq. (9) decreased with increase in ρ_{BQ} as shown in Fig. 4(c). Therefore, the IPCE value decreased with decrease in L. This result shows that an electron injected from **N719** to TiO_2 is

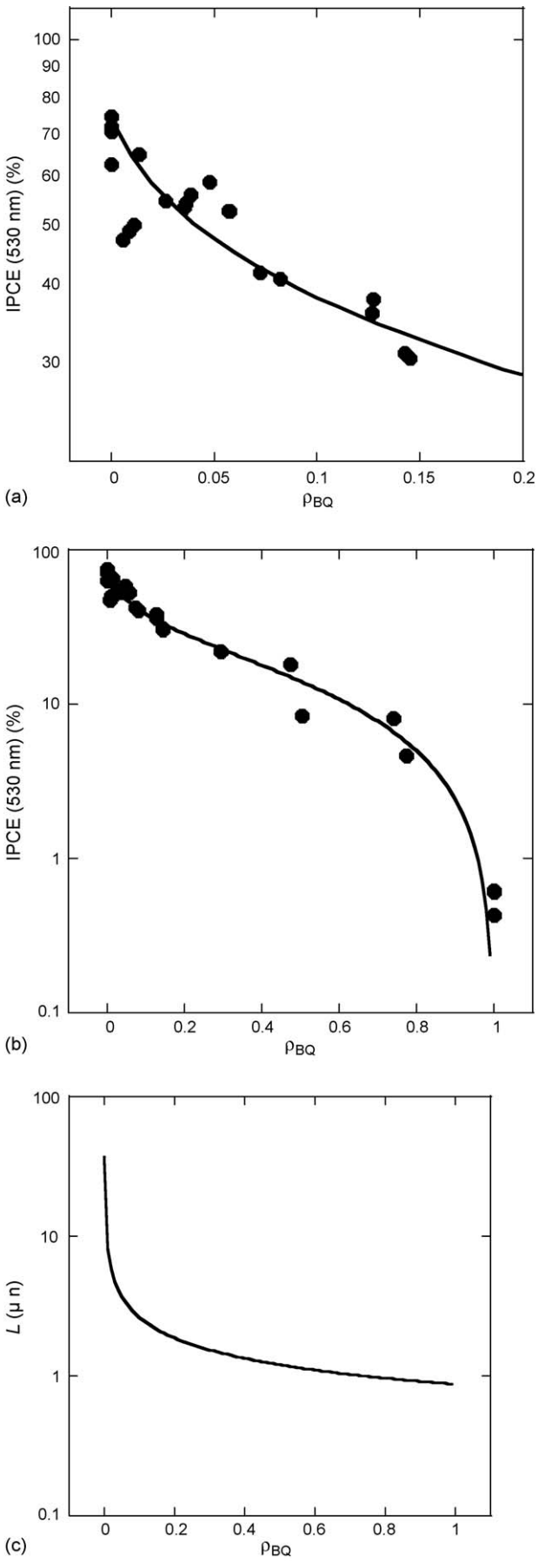

Fig. 4. Incident monochromatic photon-to-current conversion efficiency (IPCE in %) value at 530 nm for DSCs based on nanocrystalline TiO_2 with co-adsorbed **BQ** and **N719**. The ratio ρ_{BQ} is defined as $\Gamma_{BQ}/(\Gamma_{BQ} + \Gamma_{N719})$, where Γ_{BQ} and the Γ_{N719} are the amounts of **BQ** and **N719** adsorbed on the TiO_2, respectively. The lines of IPCE versus ρ_{BQ} were calculated from Eqs. (8) and (9) for values of k_{trap} and σ_{trap} of 1800 $cm^3\ s^{-1}$ and 1.1, respectively. (a) IPCE versus ρ_{BQ} at $0 \leq \rho_{BQ} \leq 0.2$. (b) log(IPCE) versus ρ_{BQ} at $0 \leq \rho_{BQ} \leq 1$. (c) Diffusion length (L) versus ρ_{BQ} calculated from Eq. (9) at $k_{trap} = 1800\ cm^3\ s^{-1}$ and $\sigma_{trap} = 1$.

substantially trapped in **BQ** on TiO_2. From intensity-modulated photocurrent spectroscopy (IMPS) at short-circuit, k_{trap} and σ_{trap} at $J_{sc}d^{-1} = 7.5 \times 10^2$ mA cm^{-3} were estimated to be 75 cm^3 s^{-1} and 20, respectively [32]. Eqs. (9) and (18) cannot fully explain the plot of IPCE versus ρ_{BQ}, because L, D, k_{trap}, and σ_{trap} also depend on the electron density (n) or J_{sc} in TiO_2. The n-dependent L, D, k_{trap}, and σ_{trap} are neglected in Eqs. (9) and (18).

4.3. Dark current

An electron cannot be injected from the conductive material to the TiO_2 bulk crystalline electrode at the ohmic interface until the applied potential is more negative than E_{cb}. The onset of the potential for a dark current has been approximated to be the E_{cb} for bulk crystalline electrodes. However, dark current has been observed at potentials more positive than E_{cb}. The dark current increased with increasing d. Therefore, we assumed that electrons are injected from the conductive glass to the TiO_2 through trap sites in the TiO_2. The trapped electrons diffuse among the trap sites in the TiO_2. The trapped electrons reach the surface of the TiO_2 and react with I_2. When **BQ** is adsorbed on the TiO_2, the dark current substantially increased with increasing ρ_{BQ}.

According to electrochemical impedance measurements, the dark current–bias curves of DSCs (Fig. 5(a)) show the influence of many processes: resistance of the conductive glass, the reverse electron rate from TiO_2 to I_2, the electron diffusion, the diffusion of I^- and I_3^-, and the I^-/I_3^- redox reaction on Pt [37]. The reaction of $I_3^- + 2e^- \rightarrow 3I^-$ also depends on n [18]. In addition, the value of D_{app} increases with increasing bias (the negative shift of the quasi Fermi level in TiO_2) because the n value increases with increasing bias [38]. Therefore, analyzing the dark current–bias curves of DSCs is difficult. The dark current–bias curves were calculated from Eq. (14) at $k_{trap} = 1800$ cm^3 s^{-1}, $\sigma_{trap} = 1.1$, $m = 1$, $N_c = 3.1 \times 10^{21}$ [39], and $E_{cb} - E(I_3^-/I^-) = 0.95$ [39]. Fig. 5(b) suggests that the dark current shown in Fig. 5(a) clearly depends on ρ_{BQ}. The increase in dark current is mainly due to the increase in the reverse electron rate from TiO_2 to I_2.

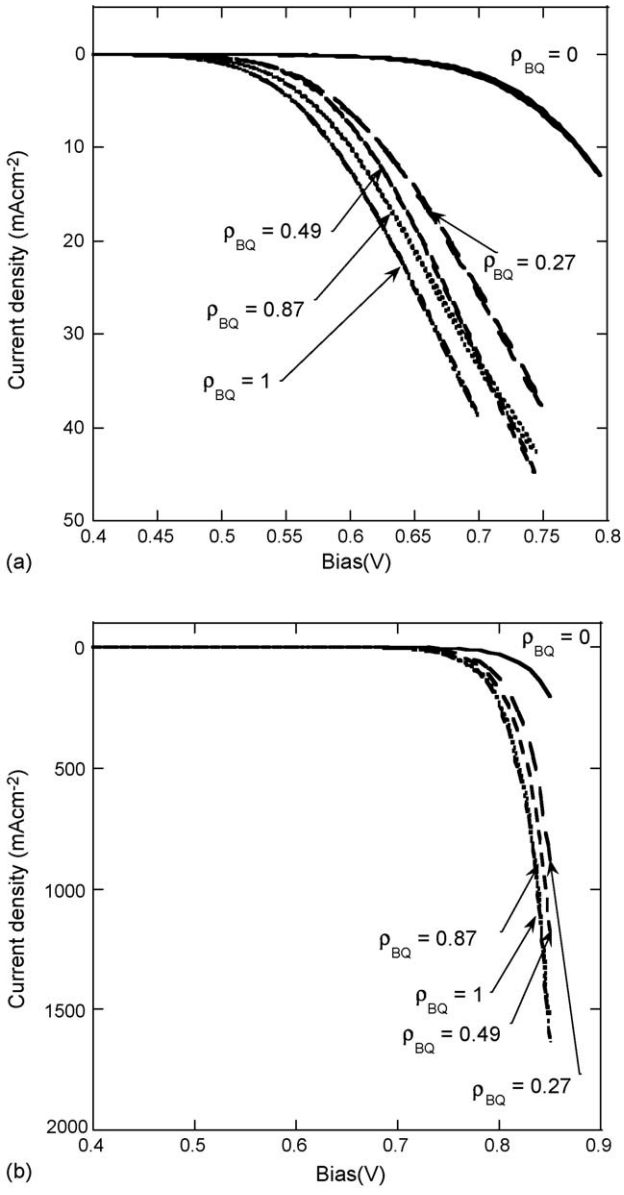

Fig. 5. (a) Dark current–bias characteristics of DSCs based on nanocrystalline TiO_2 with co-adsorbed **BQ** and **N719**. (b) Dark current–bias curve calculated from Eq. (14) at $k_{trap} = 1800$ cm^3 s^{-1}, $\sigma_{trap} = 1.1$, $N_c = 3.1 \times 10^{21}$ [39], and $E_{cb} - E(I_3^-/I^-) = 0.95$ [39].

4.4. Open circuit photovoltage (V_{oc})

From Eqs. (16) and (17), the V_{oc} can be represented by

$$V_{oc} = \frac{mkT}{q} \ln\left(\frac{J_{sc}\tau_{app}/d}{qn_0 L/d \tanh(d/L)}\right). \quad (22)$$

The V_{oc} has information about E_{cb} and τ_{app}. When at L is much larger than d ($L \gg d$), Eq. (22) can be simplified as

$$V_{oc} = \frac{mkT}{q} \ln\left(\frac{J_{sc}\tau_{app}}{qn_0 d}\right) \quad (23)$$

When the τ_{app} values of DSCs are identical, we can estimate the shift of E_{cb}. We found that E_{cb} of TiO_2 sensitized with $[NBu_4]_2[Ru(Htcterpy)(NCS)_3]$ was more positive than that sensitized with **N719** [31]. The V_{oc} is well correlated with dark current at the same J_{sc} value (or same n value). Eq. (23) can be also described as follows:

$$V_{oc} = \frac{mkT}{q} \ln\left(\frac{J_{sc}\tau_{app}}{d}\right) - \frac{mkT}{q} \ln(qn_0). \quad (24)$$

The $J_{sc}\tau_{app}$ dependent V_{oc} values are shown in Fig. 6. The J_{sc} values are proportional to the photon flux (I_b) of the bias light. Because the J_{sc} values are also proportional to d when $d < 10$ μm, the J_{sc} values were normalized at d. The τ_{app} values of DSCs with co-absorbed **BQ** and **N719** estimated from IMVS decreased with increasing ρ_{BQ} [32]. The n_0 values can be calculated from the intercept of the plot in Fig. 6. The ratio of n_0 at $\rho_{BQ} = 0.04$ to that at $\rho_{BQ} = 0$ was 0.0123. We assumed that the n_0 values were constant for ρ_{BQ} values except for $\rho_{BQ} = 0$. The apparent

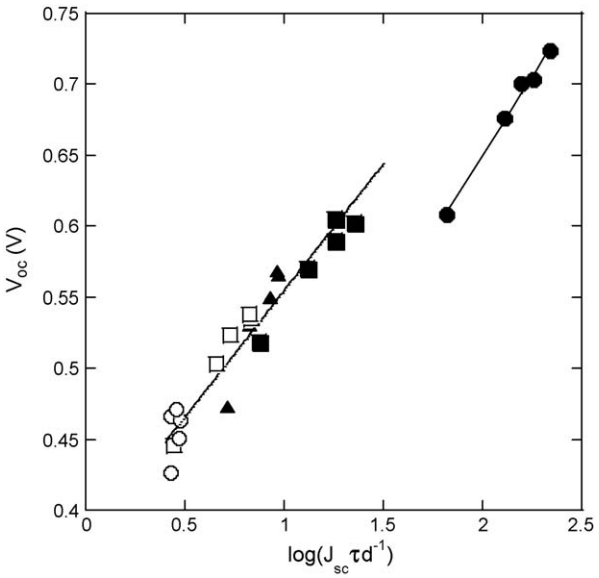

Fig. 6. V_{oc} versus $J_{sc}\tau_{app}d^{-1}$ for $\rho_{BQ}=0$ (●), 0.04 (■), 0.13 (▲), 0.30 (□), and 1 (○).

L values under open circuit conditions decrease with increasing ρ_{BQ}.

5. Conclusion

The photovoltaic performance of dye-sensitized solar cells (DSCs) based on nanocrystalline TiO_2 films with co-absorbed $[NBu_4]_2$[*cis*-Ru(Hdcbiq)$_2$(NCS)$_2$] (**BQ**; $[NBu_4]^+$ = tetrabutyl ammonium cation; H_2dcbiq = 4,4′-dicarboxy-2,2′-biquinoline) and $[NBu_4]_2$[*cis*-Ru(Hdcbpy)$_2$(NCS)$_2$] (**N719**; H_2dcbpy = 4,4′-dicarboxy-2,2′-bipyridine) has been investigated. The excited state (E^*_{ox}) of **BQ** is more positive than that of **N719** and is comparable to the conduction band edge (E_{cb}) of TiO_2 [14,32]. We have proposed that an electron injected from **N719** to TiO_2 and then trapped by **BQ** subsequently reacted with I_2 [32]. The short circuit photocurrent density (J_{sc}), open circuit photovoltage (V_{oc}), and dark current of DSCs with co-absorbed **BQ** and **N719** can be explained by the reverse electron transfer from TiO_2 to I_2 through **BQ**.

The IPCE values of TiO_2 with co-absorbed **BQ** and **N719** were smaller than the value for **N719**-sensitized TiO_2. The dark current increased with increasing ρ_{BQ}. The V_{oc} values of TiO_2 with co-absorbed **BQ** and **N719** were smaller than the value for **N719**-sensitized TiO_2. We considered that the L value decreases with increasing ρ_{BQ}. The IPCE decreased substantially even when a small amount of **BQ** was co-adsorbed with **N719** on TiO_2. Interactions between **N719** and **BQ**, such as electron transfer and energy transfer, seem to be negligible. Therefore, the η_{inj} does not depend on ρ_{BQ}. The injected electron must be rapidly trapped by **BQ** on TiO_2. The diffusion length (L) values are influenced by the electrolytes and by structural characteristics of the TiO_2 film such as the particle size, the distribution of particle sizes, the porosity of the film, and the electronic conditions at the grain boundary [15–25,27]. These results show that L also depends on whether **BQ** is adsorbed on TiO_2. We conclude that electron transport in TiO_2 is influenced not only by TiO_2 and the electrolyte but also by the presence of a sensitizer on the TiO_2.

Acknowledgment

This work was supported by a Grant-in-Aid for Young Scientists (B) from the Japan Society for the Promotion of Science (JSPS).

References

[1] B. O'Regan, M. Grätzel, Nature 353 (1991) 737.
[2] Md.K. Nazeeruddin, A. Kay, I. Rodicio, R. Humphry-Baker, E. Müller, P. Liska, N. Vlachopoulos, M. Grätzel, J. Am. Chem. Soc. 115 (1993) 6382.
[3] Md.K. Nazeeruddin, S.M. Zakeeruddin, R. Humphry-Baker, M. Jirousek, P. Liska, N. Vlachopoulos, V. Shklover, C.-H. Fischer, M. Grätzel, Inorg. Chem. 38 (1999) 6298.
[4] Md.K. Nazeeruddin, P. Péchy, M. Grätzel, Chem. Commun. (1997) 1705.
[5] Md.K. Nazeeruddin, P. Péchy, T. Renouard, S.M. Zakeeruddin, R. Humphry-Baker, P. Comte, P. Liska, L. Cevey, E. Costa, V. Shklover, L. Spiccia, G.B. Deacon, C.A. Bignozzi, M. Grätzel, J. Am. Chem. Soc. 123 (2001) 1613.
[6] A. Islam, H. Sugihara, K. Hara, R. Katoh, S. Murata, H. Arakawa, New J. Chem. 26 (2002) 966.
[7] A. Islam, H. Sugihara, K. Hara, L.P. Singh, R. Katoh, M. Yanagida, Y. Takahashi, S. Murata, H. Arakawa, J. Photochem. Photobiol. A 145 (2001) 135.
[8] R. Argazzi, C.A. Bignozzi, T.A. Heimer, F.N. Castellano, G.J. Meyer, Inorg. Chem. 33 (1994) 5741.
[9] T.A. Heimer, E.J. Heilweil, C.A. Bignozzi, G.J. Meyer, J. Phys. Chem. A 104 (2000) 4256.
[10] A. Islam, K. Hara, L.P. Singh, R. Katoh, M. Yanagida, S. Murata, Y. Takahashi, H. Sugihara, H. Arakawa, Chem. Lett. (2000) 490.
[11] A. Islam, H. Sugihara, L.P. Singh, K. Hara, R. Katoh, Y. Nagawa, M. Yanagida, Y. Takahashi, S. Murata, H. Arakawa, Inorg. Chim. Acta 322 (2001) 7.
[12] M. Yanagida, T. Yamaguchi, M. Kurashige, G. Fujihashi, K. Hara, R. Katoh, H. Sugihara, H. Arakawa, Inorg. Chim. Acta 351 (2003) 283.
[13] M. Yanagida, A. Islam, Y. Tachibana, G. Fujihashi, R. Katoh, H. Sugihara, H. Arakawa, New J. Chem. 26 (2002) 963.
[14] M. Yanagida, T. Yamaguchi, M. Kurashige, K. Hara, R. Katoh, H. Sugihara, H. Arakawa, Inorg. Chem. 42 (2003) 7921.
[15] L. Dloczik, O. Ileperuma, I. Lauermann, L.M. Peter, E.A. Ponomarev, G. Redmond, N.J. Shaw, I. Uhlendorf, J. Phys. Chem. B 101 (1997) 10281.
[16] L.M. Peter, D. Vanmaekelbergh, in: R.C. Aklire, D. Kolb (Eds.), Advances in Electrochemical Science and Engineering, vol. 6, Wiley-VCH, Weinheim, 1999, pp. 77–163.
[17] L.M. Peter, E.A. Ponomarev, G. Franco, N. Shaw, J. Electrochim. Acta 45 (1999) 549.
[18] A.C. Fisher, L.M. Peter, E.A. Ponomarev, A.B. Walker, K.G.U. Wijayantha, J. Phys. Chem. B 104 (2000) 949.
[19] G. Schlichthörl, S.Y. Huang, J. Sprague, A.J. Frank, J. Phys. Chem. B 101 (1997) 8141.
[20] G. Schlichthörl, N.G. Park, A.J. Frank, J. Phys. Chem. B 103 (1999) 782.
[21] R. Kern, R. Sastrawan, J. Ferber, R. Stangl, L. Luther, Electrochim. Acta 47 (2002) 4213.
[22] S. Nakade, M. Matsuda, S. Kambe, Y. Saito, T. Kitamura, T. Sakata, Y. Wada, H. Mori, S. Yanagida, J. Phys. Chem. B 106 (2002) 10004.
[23] S. Nakade, Y. Saito, W. Kubo, T. Kitamura, Y. Wada, S. Yanagida, J. Phys. Chem. B 107 (2003) 8607.
[24] S. Nakade, W. Kubo, Y. Saito, T. Kanzaki, T. Kitamura, Y. Wada, S. Yanagida, J. Phys. Chem. B 107 (2003) 14244.

[25] S. Nakade, T. Kanzaki, W. Kubo, T. Kitamura, Y. Wada, S. Yanagida, J. Phys. Chem. B 109 (2005) 348.
[26] S. Nakade, Y. Saito, W. Kubo, T. Kanzaki, T. Kitamura, Y. Wada, S. Yanagida, Electrochem. Commun. 5 (2003) 804.
[27] M. Yanagida, K. Miyamoto, K. Sayama, K. Kasuga, M. Kurashige, S. Takano, G. Fujihashi, Y. Abe, H. Sugihara, Electrochim. Acta 51 (2006) 3993.
[28] J.N. Clifford, G. Yahioglu, L.R. Milgrom, J.R. Durrant, Chem. Commun. 12 (2002) 1260.
[29] P.G. Hoertz, D.W. Thompson, L.A. Friedman, G.J. Meyer, J. Am. Chem. Soc. 124 (2002) 9690.
[30] K. Hara, K. Miyamoto, Y. Abe, M. Yanagida, J. Phys. Chem. B 109 (2005) 23776.
[31] K. Miyamoto, M. Yanagida, K. Sayama, H. Sugihara, Y. Abe, Chem. Lett. 35 (2006) 336.
[32] M. Yanagida, K. Miyamoto, K. Sayama, K. Kasuga, M. Kurashige, Y. Abe, H. Sugihara, J. Phys. Chem. B, submitted for publication.
[33] C.J. Barbé, F. Arendse, P. Comte, M. Jirousek, F. Lenzmann, V. Shklover, M. Grätzel, J. Am. Ceram. Soc. 80 (1997) 3157.
[34] B.J. Walter, C.M. Elliott, Inorg. Chem. 40 (2001) 5924.
[35] S. Södergren, A. Hagfeldt, J. Olsson, S.-E. Lindquist, J. Phys. Chem. 98 (1994) 5552.
[36] V. Shklover, Y.E. Ovchinnikov, L.S. Braginsky, S.M. Zakeeruddin, M. Grätzel, Chem. Mater. 10 (1998) 2533.
[37] L. Han, N. Koide, Y. Chiba, T. Mitate, Appl. Phys. Lett. 84 (2004) 2433.
[38] F. Fabregat-Santiago, J. Bisquert, G. Garcia-Belmonte, G. Boschloo, A. Hagfeldt, Sol. Energy Mater. Sol. Cells 87 (2005) 117.
[39] A. Usami, Chem. Phys. Lett. 292 (1998) 223.